◆ Human Brain Mapping 37:311–326 (2016) ◆

Cortical Localization of Phase and Amplitude Dynamics Predicting Access to Somatosensory Awareness

Jonni Hirvonen[1,2] **and Satu Palva**[1]*

[1]*Neuroscience Center, University of Helsinki, Finland*
[2]*BioMag Laboratory, HUS Medical Imaging Center, Finland*

Abstract: Neural dynamics leading to conscious sensory perception have remained enigmatic in despite of large interest. Human functional magnetic resonance imaging (fMRI) studies have revealed that a co-activation of sensory and frontoparietal areas is crucial for conscious sensory perception in the several second time-scale of BOLD signal fluctuations. Electrophysiological recordings with magneto- and electroencephalography (MEG and EEG) and intracranial EEG (iEEG) have shown that event related responses (ERs), phase-locking of neuronal activity, and oscillation amplitude modulations in sub-second timescales are greater for consciously perceived than for unperceived stimuli. The cortical sources of ER and oscillation dynamics predicting the conscious perception have, however, remained unclear because these prior studies have utilized MEG/EEG sensor-level analyses or iEEG with limited neuroanatomical coverage. We used a somatosensory detection task, magnetoencephalography (MEG), and cortically constrained source reconstruction to identify the cortical areas where ERs, local poststimulus amplitudes and phase-locking of neuronal activity are predictive of the conscious access of somatosensory information. We show here that strengthened ERs, phase-locking to stimulus onset (SL), and induced oscillations amplitude modulations all predicted conscious somatosensory perception, but the most robust and widespread of these was SL that was sustained in low-alpha (6–10 Hz) band. The strength of SL and to a lesser extent that of ER predicted conscious perception in the somatosensory, lateral and medial frontal, posterior parietal, and in the cingulate cortex. These data suggest that a rapid phase-reorganization and concurrent oscillation amplitude modulations in these areas play an instrumental role in the emergence of a conscious percept. *Hum Brain Mapp 37:311–326, 2016.*

Key words: MEG; somatosensory; conscious; perception; source; oscillation; cortex

Additional Supporting Information may be found in the online version of this article.

Contract grant sponsors: The Academy of Finland, University of Helsinki Research Grants, Research Foundation of the University of Helsinki, and Sigrid Juselius Foundation; Contract grant numbers: SA 1126967 and SA 266402

*Correspondence to: Satu Palva, Neuroscience Center, University of Helsinki, Finland. E-mail: satu.palva@helsinki.fi

Received for publication 9 April 2015; Revised 2 October 2015; Accepted 6 October 2015.

DOI: 10.1002/hbm.23033
Published online 20 October 2015 in Wiley Online Library (wileyonlinelibrary.com).

INTRODUCTION

Despite large interest and accumulating knowledge, the anatomical patterns of subsecond scale neuronal correlates of consciousness (NCC) have remained enigmatic. Theoretical models of sensory awareness suggest that neuronal activity in sensory regions high in hierarchy, as well as in frontal and parietal areas forming a frontoparietal (FP) network [Dehaene et al., 2006; Dehaene and Changeux, 2011] as well as recurrent processing within sensory cortices and between sensory cortices and frontoparietal areas [Lamme, 2006; Lamme and Roelfsema, 2000; van Gaal and Lamme, 2012] are crucial constituents of sensory awareness. Neuronal mechanisms underlying conscious perception can be investigated by presenting subjects sensory stimuli with intensity at the verge of detection and for which perceived and unperceived conditions alternate intermittently [Aru et al., 2012; Hansen et al., 2004; Monto et al., 2008a; Palva et al., 2005; Pins and Ffytche, 2003; Vidal et al., 2014; Wyart and Tallon-Baudry, 2008, 2009]. In line with the theoretical suggestions both functional MRI (fMRI) [Boly et al., 2011; Haynes et al., 2005b; Marois et al., 2004; Vuilleumier et al., 2001] and lesion [Del Cul et al., 2009; Vuilleumier et al., 2001] studies indeed show that activity in frontoparietal areas but also in sensory areas higher in processing hierarchy such as in occipitotemporal cortex [Bar et al., 2001; Grill-Spector et al., 2000; Hesselmann and Malach, 2011; Hesselmann et al., 2011; Kouider et al., 2007; Polonsky et al., 2000; Tong et al., 1998] is increased and correlated positively with conscious perception. Further, also activity in insula, anterior and posterior cingulate cortices, and thalamus [Boly et al., 2007; Marois et al., 2004; Sadaghiani et al., 2009] predicts whether sensory stimuli will be consciously detected. Thus, in the multi-second time scales of the BOLD signal fluctuations, conscious access is correlated with increased activity levels in the frontoparietal control areas belonging functionally to FP and dorsal attention networks (DAN) but also with the activity-levels in the ventral attention (VAN) and default-mode network (DMN), which signal the salience or bottom-up attention to the sensory stimuli [Corbetta and Shulman, 2002; Dosenbach et al., 2008; Power et al., 2011] and self-oriented behaviors [Michelet et al., 2015; Nagels et al., 2015; Sheth et al., 2012], respectively.

Electrophysiological recordings reveal neuronal activity with millisecond precision and can hence be used to complement the insight obtained with fMRI by elucidating the sub-second time-scale correlates of conscious sensory perception. Both non-invasive EEG [Del Cul et al., 2007; Fahrenfort et al., 2007; Koivisto et al., 2008; Pins and Ffytche, 2003; Sergent et al., 2005], and MEG [Jones et al., 2007; Melloni et al., 2011; Palva et al., 2005] data as well as iEEG recordings [Fisch et al., 2009; Gaillard et al., 2009] show that the strength of evoked responses (ER) is positively correlated with conscious sensory perception. In addition to ER, also neuronal oscillations and their phase and amplitude dynamics, which regulate neuronal information processing [Cardin et al., 2009; Singer, 1999; Womelsdorf and Fries, 2007], are predictive of whether sensory stimuli are consciously perceived.

Both MEG sensor-level analyses [Palva et al., 2005; Wyart and Tallon-Baudry, 2008] and iEEG [Aru et al., 2012; Fisch et al., 2009; Gaillard et al., 2009; Vidal et al., 2014, 2015] studies have shown that specifically the amplitudes of local gamma ($30-120$ Hz) oscillations are correlated with conscious perception of visual stimuli. Yet, although the strength of local gamma oscillations is correlated with awareness, it has been shown using iEEG recordings that the strength of gamma oscillations reflects also visual processing per se rather than merely the conscious perception [Aru et al., 2012; Vidal et al., 2014], which implies that the neural correlates of conscious perception are complex and cannot be attributed to any simple parameter such as the strength of high-frequency oscillations. Our prior study on somatosensory awareness has indeed shown that although the strength of local gamma oscillations is correlated with conscious somatosensory perception, this modulation was observed with concurrent stimulus phase-locking of ongoing alpha ($8-14$ Hz) oscillations [Palva et al., 2005]. The strength of alpha-band oscillations in extra-striate visual regions is also positively correlated with visual awareness [Vidal et al., 2015] as well as with the subjective experience of the perceptual awareness [Auksztulewicz and Blankenburg, 2013] suggesting that conscious sensory perception is due to concurrent neuronal activity in many frequency bands. In line with the idea of a complex hierarchical cascade of neuronal processing leading to the conscious perception, the poststimulus oscillatory correlates of conscious somatosensory perception are complemented by observations showing that also the prestimulus amplitude of alpha-band oscillations is correlated with conscious somatosensory perception either with a quadratic [Linkenkaer-Hansen et al., 2004] or a negative linear [Jones et al., 2010] relationship as well as that the mutual connectivity of sensory, cingulate, and insular regions before stimulus presentation is positively correlated with subsequent predictions [Sadaghiani et al., 2015]

However, as most EEG and MEG studies investigating neuronal correlates of sensory awareness have been conducted with scalp-sensor-level rather than with source-reconstructed data, the cortical areas where the neuronal phase- and amplitude dynamics are predictive of conscious sensory perception in these recordings have remained obscure. In line, iEEG recordings have limited sparse cortical coverage and have observed positive correlation of oscillation dynamics and conscious visual perception in large-areas over the visual cortex, but have not revealed whether such correlation would be observed also in frontal cortex and salience networks.

To investigate in which cortical regions the electrophysiological markers are predictive of the subsequent conscious access of somatosensory stimuli as well as to

identify the cascade of frequency resolved dynamics of such neuronal phase and amplitude modulations and ER leading to conscious perception, we recorded magnetoencephalography (MEG) during a somatosensory threshold-stimulus detection task and used state-of-the-art source localization and data analysis methods to localize neuroanatomical sources of local cortical phase- and amplitude dynamics and evoked responses.

MATERIAL AND METHODS

Subjects and Recordings

Brain activity was recorded from 15 healthy right-handed subjects (23–32 years of age; seven females) with a 306 channel MEG instrument composed of 204 planar gradiometers and 102 magnetometers (Elekta Neuromag, Helsinki, Finland) at 600 Hz sampling rate. Three subjects were excluded from the analysis because of excessive sensor noise. Electromyogram (EMG) was recorded to detect the subjects' responses given by thumb movement. T1-weighted anatomical magnetic resonance imaging (MRI) scans were obtained for each subject at a resolution of a $\leq 1 \times 1 \times 1$ mm (MP-RAGE) with a 1.5 T MRI scanner (Siemens, Germany). The study was approved by an ethical committee of the Helsinki University Central Hospital and the subjects gave written informed consents on participation in the experiment.

Experimental Protocol

We used a continuous threshold-stimulus detection task (TSDT) where electrical stimuli were given with an intensity at the threshold of detection [Monto et al., 2008a; Palva and Palva, 2011; Palva et al., 2005]. Stimuli were delivered with a constant-current stimulator and plate electrodes at random 1.5 to 4.5 s intervals to the distal part of the right or both index fingers in separate blocks. Before each recording session, the intensity was separately adjusted for both fingers so that the detection rate was ~50%. During the recording sessions, the stimulus intensity was kept constant. The mean stimulus current was 4.3 ± 0.6 mA and the stimulus duration was 0.2 ms. Two 30 min sessions were recorded for both the right-hand and both-hands (bimanual) stimulation conditions. For the present analyses, we used only the data from the two blocks with one-hand right index finger stimulation for which $1{,}073 \pm 207$ (mean ± standard deviation, SD) trials were obtained. No trials were rejected. During the recording sessions, subjects sat relaxed with their eyes closed and were instructed to promptly twitch the thumb of the hand(s) in which they felt the stimulus. The thumb twitches were recorded with EMG with electrodes placed on the abductor/flexor pollicis brevis and detected off-line from band-pass (50 − 150 Hz) filtered data.

Behavioral Performance

Hit rate (HR) was estimated as the proportion of correct responses from all right-hand stimuli. The latency at which the EMG burst exceeded 10 baseline (BL) SDs was defined as the reaction time (RT) [Monto et al., 2008a; Palva et al., 2005]. A stimulus followed by a correct response 0.1–1.5 s after the onset was categorized as consciously perceived (Hit) and a stimulus to which no response was observed was categorized as unperceived (Miss). Other stimulus–response combinations (e.g. incorrect or delayed responses and false alarms) were not analyzed because of the exceedingly small number of trials in these categories. We obtained $1{,}073 \pm 207$ (mean ± standard deviation, SD) trials for each subject of which 411 ± 164 trials were Hits. The number of trials between the Hit and the Miss conditions were balanced for each subject before the analyses.

Analysis of Behavioral Clustering

The time-series of behavioral data was analyzed for long-range temporal correlations (LRTCs) that measure the underlying temporal clustering of Hits and Misses. We applied detrended fluctuation analysis (DFA) to estimate the scaling laws for the long-range temporal correlation of the Hit-Miss sequence as in Palva et al. [2013]. Briefly, the behavioral time series were linearly interpolated into a time series of 0 s and 1s with a sampling rate of 10 Hz. DFA was then performed on these data and to discard any possible effects of this interpolation on the scaling law exponents, only the DFA time windows between 4 and 400 s were used in the regression. To confirm that the behavioral LRTCs could not be explained by a random process, we shuffled the Hit-Miss time series and re-estimated the DFA scaling exponents for 20 randomizations. The difference between the surrogate mean and real data was tested with a paired *t*-test across the subjects.

MEG Data Preprocessing, Filtering, Source Analysis, and Surface Parcellations

We first preprocessed the raw MEG time series with the temporal extension of signal space separation method (SSS) [Taulu et al., 2005] which was used to remove extracranial noise from the raw MEG recordings and to co-localize the recordings across sessions and subjects. Next, independent component analysis (ICA) [Bell and Sejnowski, 1995] was used to identify and exclude components associated with eyes movements/blinks and cardiac artifacts. The preprocessed MEG time-series data from each separate channel was then narrow-band filtered into 31 frequency bands, $f_{min} = 3$ Hz; $f_{max} = 120$ Hz by convolving the sampled MEG signals with a family of Morlet wavelets $w(t, f_0)$, $w(t, f_0) = A\exp(-t^2/2\sigma_t{}^2 \; 2)\exp(2i\pi f_0 t)$, where $\sigma_t = m/2\pi f_0$, i is the imaginary unit, m (=5) defines the

compromise between time and frequency resolution, and f_0 is the center frequency of the wavelet [Palva et al., 2005]. The convolution $X(t,f_0) = x(t) \times w(t,f_0)$ gives a complex vector $X(t,f_0)$, of which the angle is the phase of the signal x in a frequency band with a center frequency of f_0 and a frequency-domain SD of $\sigma_f = f_0/m$ [Tallon-Baudry et al., 1996]. Finite impulse-response filter was used for broad-band filtering from 0.1 to 45 Hz (pass-band from 1 to 40 Hz) and Hilbert-transformation to obtain the signal phase time series [Palva et al., 2013].

We used FreeSurfer software (http://surfer.nmr.mgh.harvard.edu/) for automatic volumetric segmentation of the MRI data, surface reconstruction, flattening, cortical parcellation, and labeling with the Freesurfer/Destrieux atlas [Dale et al., 1999; Destrieux et al., 2010; Fischl et al., 2002]. MNE software (http://www.nmr.mgh.harvard.edu/martinos/userInfo/data/sofMNE.php) was used to create three-layer boundary element models (BEM), cortically constrained source models, MEG-MRI co-localization and for preparation of the forward model and inverse operators [Hämäläinen and Ilmoniemi, 1994; Hämäläinen and Sarvas, 1989]. The source models had dipole orientations fixed to the pial surface normals and a 7 mm source-to-source separation throughout the cortex, which yielded models containing 6,000 to 8,000 source vertices. To reconstruct ongoing cortical dynamics, we used minimum-norm estimate (MNE) inverse operators in the form of dynamic statistical parametric map (dSPM) operators [Dale et al., 2000] that were built by computing noise-covariance matrices from the baseline data from 0.75 to 0.2 before stimulus onset and using 0.05 as the regularization constant separately for the broad-band and each wavelet filter frequency by using noise covariance matrices that were filtered (broad-band and wavelet, respectively) from the prestimulus baseline period of all trials. We then collapsed source time-series to time series of 400 cortical parcels from a precursor atlas of 148 parcels [Destrieux et al., 2010] by iteratively splitting the largest parcels of the Destrieux atlas along their most elongated axis using the same parcel-wise splits for all subjects. Using neuroanatomical labeling as the anatomical "coordinate system" eliminates the need for intersubject morphing in group-level analyses which would have compromised individual anatomical accuracy [Honkanen et al., 2014; Palva et al., 2010, 2011]. The selection of source vertices to cortical parcels was performed with sparse weighted collapse operators that maximized the source reconstruction accuracy for each subject's source space [Korhonen et al., 2014].

Analysis of Evoked Responses, Oscillation Amplitudes, and Phase-Locking to Stimulus Onset

The collapsed parcel-wise broad-band filter based inverse estimates, $X_{F,P,r}(t,f)$ of single trials r, $r = 1 \ldots n_s$, were used for cortex-wide mapping of phase locking of ongoing activity to the stimuli (stimulus locking, SL), evoked responses (ER), and induced amplitude (A) dynamics. Stimulus locking was quantified with the phase-locking value, PLF(t,f) (also known as the phase-locking factor), that was given for each parcel $a = 1 \ldots n_p$ by $\mathrm{PLF} = n_s^{-1} \left| \Sigma_r \left(x_{F,P,a} / \left| x_{F,P,a} \right| \right) \right|$ [Sinkkonen et al., 1995]. PLF yields thus values between 0 and 1, so that with an increasing number of samples, PLV approaches 0 for an uniform phase distribution. For perfect phase-locking, PLV = 1. The averaged event-related amplitude envelopes, $A(t,f)$, were given by $A = n_s^{-1}\Sigma_r \left(\left| x_{F,P,a} \right| \right)$ [Palva et al., 2005; Tallon-Baudry et al., 1996] and the evoked responses, ER(t,f), simply by the averaging the real parts of the time series so that $\mathrm{ER} = n_s^{-1}\Sigma_r \left[\mathrm{Re}(x_{F,P,a}) \right]$. $A(t,f)$, and PLF(t,f) were estimated separately for each trial type, each cortical parcel and wavelet or broad-band frequency and ER(t) only for broad-band frequency. Since in the ER the signal polarity might change in different sides of the sulci and hence across cortical parcels, we took the absolute value of the ERs before statistical analysis (see Fig. 1). It should be noted that the ER and A values in the post hoc analysis presentations (Figs. 1C and 3C,D) are dSPM values from the MNE source reconstruction rather than source currents and hence have here only a relational rather than absolute meaning.

Statistical Analyses

The group statistics across subjects and between conditions or between the prestimulus baseline and poststimulus period were performed separately for each frequency, time-window and cortical parcel. Before the statistical group analysis, the individual subject's PLF(t,f), A(t,f), and ER(t) were baseline corrected by subtracting the mean of the prestimulus period from −0.75 to −0.2 s. The significant difference of neuronal activity between Hits and Misses was estimated with the Wilcoxon signed rank test ($P < 0.05$) separately for PLF(t,f), $A(t,f)$, and ER(t) against a null hypothesis of PLF = 0, $A = 0$, and ER = 0 or $\mathrm{PLF}_{Hit} - \mathrm{PLF}_{Miss} = 0$, $A_{Hit} - A_{Miss}$ and $\mathrm{ER}_{Hit} - \mathrm{ER}_{Miss}$ as for the Hit-Miss comparison. To control the false discovery rate (FDR) in the multiple statistical comparisons performed in this study, for each contrast we pooled significant observations across all samples, frequency bands and cortical parcels and then discarded as many least-significant observations as was predicted to be false discoveries by the alpha-level used in the corresponding test [Honkanen et al., 2014; Palva et al., 2011]. In addition, for analyses of ER data, only parcels from a time-sample in a sequence of at least five consecutive same significant observations were considered significant. Statistical significance between the conditions in the behavioral data was assessed with one-way ANOVA ($P < 0.05$).

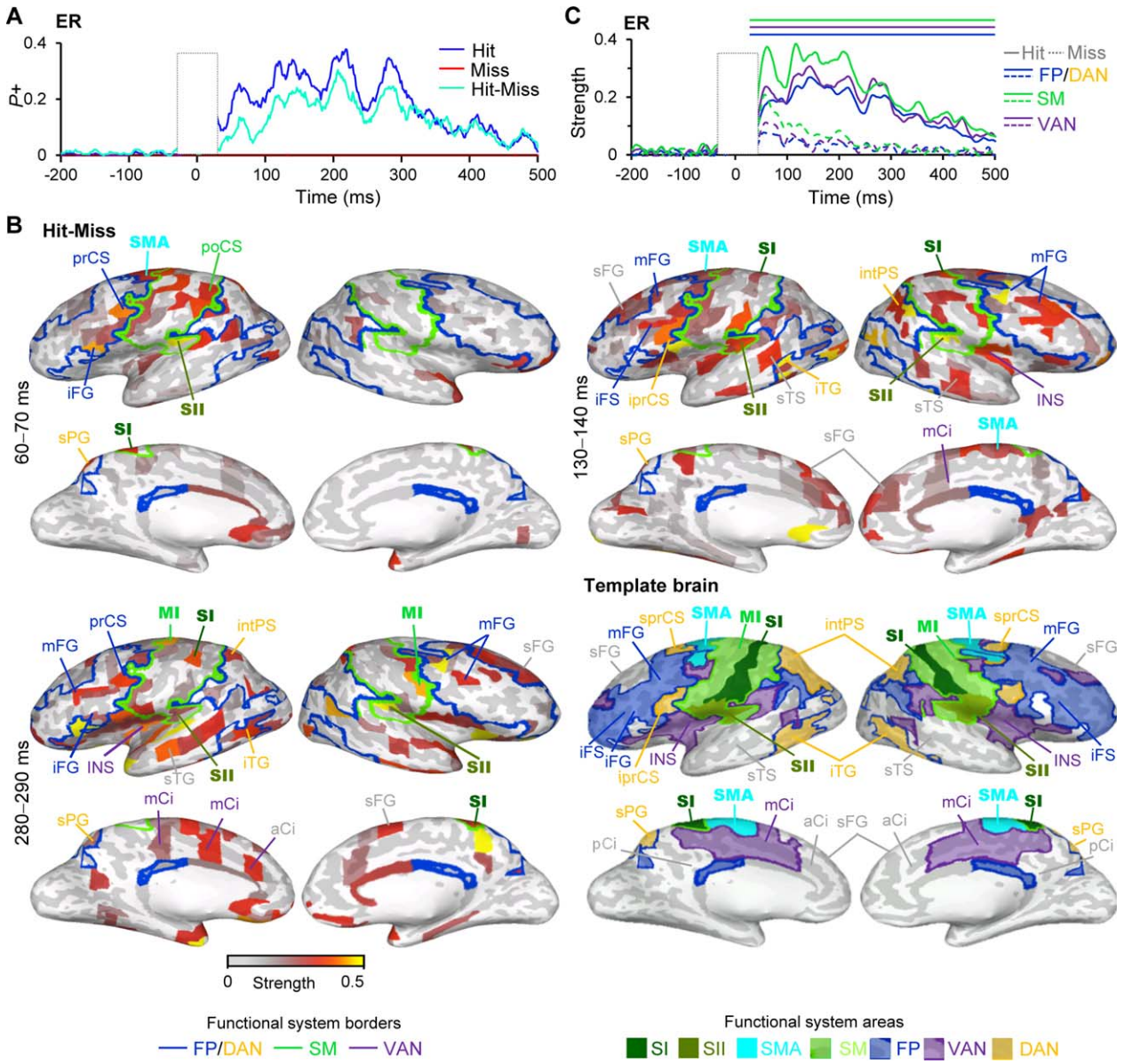

Figure 1.

Evoked responses (ER) of broad-band (1–45 Hz) filtered MEG data differ for perceived (Hit) and unperceived (Miss) stimuli. **A**) A fraction of the 400 brain areas (parcels) in which the ER was stronger ($P+$) than in the prestimulus baseline (BL) period separately for perceived stimuli (Hits (blue)) and unperceived stimuli (Misses (red)) as well as for their difference (Cyan) (Wilcoxon signed rank test, $P < 0.05$, corrected). The stimulus onset is at 0 ms. **B**) The cortical areas in which ER was stronger for Hits compared with Misses (Wilcoxon signed rank test, $P < 0.05$, FDR corrected) displayed in inflated cortical surface. Colors of the parcels indicate average strength of the ER over a selected time-window. Primary somatosensory (SI), secondary somatosensory (SII), supplementary motor area (SMA), and primary motor area (MI) are shown with bold text. Boundaries depict functional connectivity networks as identified from fMRI based functional connectivity network [Yeo et al., 2011]; frontoparietal together with dorsal attentional network (FP/DAN, blue), ventral attentional network (VAN, purple) and sensorimotor network (SM, green). Parcels are indicated with acronyms. Template brain points to the positions of functional systems and important parcels. Acronyms for the brain areas are: aCi = anterior cingulate, iprCS = inferior precentral sulcus, iFG = inferior frontal gyrus, iFS = inferior frontal sulcus, INS = insula, iTG = inferior temporal gyrus, intPS = intaparietal sulcus, mCi = middle-cingulate, mFG = middle-frontal gyrus, mFS= middle frontal sulcus, sPG = superior parietal gyrus, sTS = superior temporal sulcus, pCi = posterior cingulate, poCS = postcentral sulcus, sFG = superior frontal sulcus, sprCS = superior precentral sulcus, sPG = superior parietal gyrus, sTS = superior temporal sulcus. **C)** The relative strength of ER compared with baseline separately for Hits (solid line) and Misses (dashed line) averaged over contralateral SM (green), FP/DAN (blue), and VAN (purple). The lines above indicate significant difference between the Hit and Miss trials (Wilcoxon signed rank test, $P < 0.05$, FDR corrected).

Time-Frequency and Anatomical Visualization of the Fractions of Significant Effects

We used statistical testing across all brain regions, frequency bands, and time windows to reveal the most robust phenomena that correlated with conscious perception. To obtain a comprehensive overview of results from a given test in the time-frequency (TF) plane, we showed the fraction of parcels out of all 400 parcels with a statistically significant positive and/or negative effect (P^+_P/P^-_P). On the other hand, to reveal the brain areas accounting for the most prominent effects in the time window of interest or in a TF region of interest (TFROIs), we displayed the fraction of significant TF-elements of all elements for each anatomical parcel, visualized on a representative inflated cortical surface (P^+_{TF}/P^-_{TF}). Functional intrinsic network borders based on population level fMRI resting state activity [Yeo et al., 2011] were overlaid on the inflated surface as land markers. The parcels belonging to each network are defined in Supporting Information Table 1.

RESULTS

Behavioral Performance

To identify the neural correlates of conscious somatosensory perception, we used somatosensory threshold-stimulus detection task (TSDT) where the subjects detected weak constant-intensity electrical stimuli given to the tip of the index finger. The strength of the stimuli was calibrated to be at the threshold of detection for each subject before the recordings. After calibration, the stimulus intensity was maintained constant during the MEG recordings and the mean HRs were $38.3 \pm 15.26\%$. The mean reaction times (RTs) were 398.5 ± 135.3 ms.

Broad Band Neuronal Activity Differentiates Perceived and Unperceived Stimuli

We measured human ongoing cortical activity with MEG and used cortically-constrained minimum-norm estimates to reconstruct the underlying the cortical currents with source models matching each subjects' individual cerebral anatomy. The minimum-norm current estimates were expressed as ongoing-activity time series of cortical parcels that comprised a 400-parcel neuroanatomically labeled parcellation of the complete cortical grey matter surfaces. To investigate the neuronal activities characterizing the consciously perceived (Hits) and unperceived (Misses) somatosensory stimuli, we first quantified the strength of the absolute values of evoked responses (ER) and estimated whether the strength of ER was significantly larger or smaller than the activity during the BL period. We then estimated the proportion of cortical parcels showing either positive ($P+$) or negative ($P-$) modulations of ER separately for Hits and Misses as well as for the difference in their strengths. Hits were associated with ER showing peaks at latencies of 70 ms (M70), 130 ms (M130), 210 ms (M210), and 280 ms (M280) from stimulus onset (Fig. 1A) and were hence observed at similar latencies compared with prior studies [Jones et al., 2007; Palva et al., 2005]. Significant ER was observed in up to 37% of the cortical parcels for Hits, while for Misses ER did not differ from BL activity at the whole-brain level. ER was also stronger for Hits compared with Misses from ~70 ms onwards and showed peaks in the M130, M210, and 280 components similarly to ER for Hits (Fig. 1A).

We then identified cortical areas in which M70, M130, and M280 components were observed for Hits and for the difference between Hits and Misses. For Hits, ER was observed in the postcentral gyrus (poCG) that is the primary sensory area (SI), and in posterior part of lateral sulcus (laSp) that is the secondary somatosensory area (SII), and which both functionally belong to sensorimotor (SM) network. In addition, ERs for M70, M130, and M280 components were also observed in middle frontal gyrus (mFG) and in inferior frontal gyrus/sulcus (iFG/iFS) which correspond to dorso- and ventrolateral prefrontal cortices (dlPFC and vlPFC), respectively and also belong functionally to FP network as well as in inferior precentral sulcus (iprCS) that belongs to DAN. For M130 and M280 components, ER was observed also in intraparietal sulcus (intPS) belonging functionally to DAN and in anterior cingulate (aCi) and mid cingulate (mCi) cortices, which functionally belong to DMN and VAN, respectively (Supporting Information Fig. S1).

For M70 component, the difference in the strength of ER between Hits and Misses was salient in SI, SII, and iprCS of DAN while for M130 and M280 components ER was stronger for Hits also in supplementary motor area (SMA), in mFG, iFG, and iFS of the FP and intPS of the DAN together with mCi, aCi, and sFG of VAN and DMN, respectively (Fig. 1B). Hence for M130 and M280 components the strength of ER in dlPFC, vlPFC, and in parietal cortices, which are commonly associated with higher level cognitive processes [Fuster, 2008; Koechlin et al., 2003] and attentional control [Corbetta and Shulman, 2002; Corbetta et al., 2008] predicted conscious perception.

We then further estimated the strength of ER separately for Hits and Misses averaged over SM, FP/DAN, and VAN. This revealed that ER was stronger for the Hits than Misses in cortical parcels belonging to those networks up to 500 ms from sensory stimulus onset (Fig. 1C). As ER reflects both the amplitude of the response and its phase-locking to stimulus onset (stimulus-locking, SL), we separately investigated the influence of SL and broad-band amplitude of induced oscillations to the conscious perception with the same broad-band filter as we used for estimating ER. Both the amplitude (Fig. 2A) and SL (Fig. 2B) were larger for the Hits than Misses, although this effect was more prominent for the SL. Increased amplitude for Hits compared with Misses showed peaks at 80 to 90 ms

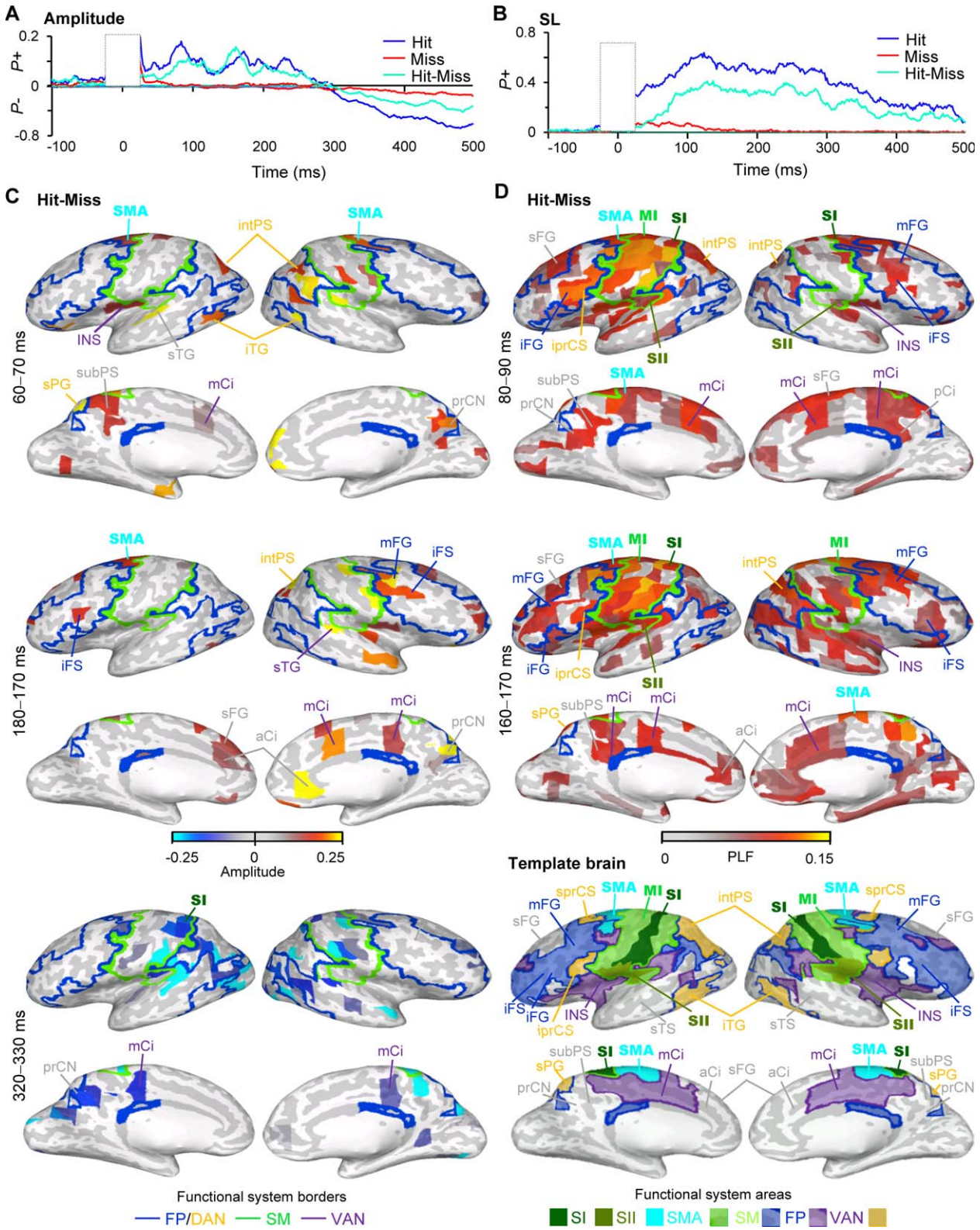

Figure 2.
(See legend on the following page.)

and 180 ms from stimulus onset, which were hence slightly later and less frequent than those of the ERs. Increased SL for Hits compared with Misses, on the other hand, did not show the peaks observed for the ER and amplitude.

Amplitude was stronger for the Hits than Misses at latency between 80 and 90 ms in contralateral SI and SII together with intPS and sPG of DAN as well as ipsilateral mFG of FP and precuneus (prCN) of VAN (Fig. 2C). At 160 to 170 ms, broad-band amplitude was increased also in iFS of FP, as well as in aCi and mCi (Fig. 2C). On the other hand, SL was stronger for the Hits than Misses in the large areas of SM network including SI and SII, throughout the frontal cortex including iFS/iFG, mFG, and sFG belonging to vlPFC and dlPFC, respectively, intPS of DAN, as well as in aCi, posterior cingulate (pCi) and precuneus (Fig. 2D).

Clustering of Behavioral Performance does not Affect Stimulus Processing

In continuous threshold detection experiments, the Hits and Misses are often clustered into sequences of similar behaviors such that Hits and Misses occur in sequences [Monto et al., 2008a; Palva and Palva, 2011; Palva et al., 2013] and the presence of these clusters are correlated with the phase of infra-slow (<0.01 Hz) fluctuations that are likely to reflect gross cortical excitability fluctuations or fluctuations among task-positive and negative systems [Palva and Palva, 2012]. In the present data, Hit-Miss series of individual subjects showed clusters of Hits and Misses (Fig. 3A). We further estimated clustering of the responses by estimating the autocorrelations in the Hit-Miss behavioral series by detrended fluctuation analysis (DFA), which showed that scaling exponents for autocorrelations in real data ranged from 0.55 to 0.9 with a mean of 0.68 ± 0.05 and were thus stronger than in random data with mean scaling exponent of 0.58 ± 0.004 ($P < 0.01$, paired *t*-test) (Fig. 3B).

These data raised a question on whether the strength of ER and SL could be dependent on the position in the behavioral Hit-Miss cluster, because the cluster positions could reflect differences in the brain excitability state that are dependent on the phase of the ISFs. Hypothetically, the strength of ER and SL could thus gradually increase as a function of the position in the Hit-Miss behavioral sequence. To thus investigate whether the strength of ER and SL were affected by their position in the Hit-Miss series, we compared the broad-band responses of adjacent Hit and Miss trials with the rest of the trials (see Fig. 3A) for data averaged over contralateral SI. The strengths of ER (Fig. 3C) and SL (Fig. 3D) for the first Hit and last Miss of a behavioral Hit-Miss sequence were not significantly different from the rest of the trials and hence not affected by their position in the Hit-Miss behavioral series ($P < 0.05$, Wilcoxon signed rank test, FDR corrected) while they were considerably larger to Hits than to Misses regardless of their position ($P < 0.05$, corrected).

The Strength of Stimulus Processing is Correlated with Reaction Times

To reveal the benefit of broad-band SL and broad-band oscillation amplitude to the processing of the consciously perceived stimuli, we divided perceived trials by their RTs into three equal sized bins; fast, intermediate, and slow, and estimated the strengths of broad-band SL and amplitude separately for data in these bins in SM, FP/DAN, and VAN. These data showed that trials with fast RTs had stronger broad-band amplitude suppression (Fig. 4A) and strengthened SL (Fig. 4B) compared with trials with slow RTs. We did not observe any modulations in trials with fast vs. intermediate RTs ($P < 0.05$, Wilcoxon signed rank test, FDR corrected).

Spectral Characteristics of SL and Induced Oscillation Amplitudes Characterizing Conscious Perception

To resolve the spectral properties of neuronal activity characterizing the Hits and Misses, we next investigated SL and oscillation amplitudes in the time-frequency (TF) domain. This analysis revealed wideband SL for both the Hits and Misses compared with BL (Fig. 5A). Hits were characterized by prominent SL centered between delta ($\delta, < 4$ Hz) and high beta- (high-β, $20 - 30$ Hz) bands and

Figure 2.

Broad-band amplitude (A) and stimulus-locking (SL) are stronger for Hits than for Misses. **A)** Fraction of brain areas (parcels) in which the amplitude of broad-band activity was stronger ($P+$) or weaker ($P-$) than in the prestimulus baseline separately for Hits (blue), Misses (red) and for their difference (cyan) (Wilcoxon signed rank test, $P < 0.05$, corrected). **B)** Fraction of brain areas (parcels) in which the phase-locking of broad-band activity to stimulus onset (stimulus-locking, SL) was stronger ($P+$) than in the prestimulus baseline. **C)** The cortical areas in which the broad-band amplitude was stronger for Hits than for Misses (Wilcoxon signed rank test, $P < 0.05$, FDR corrected) displayed in inflated cortical surface. Color indicates the average amplitude values in the selected time-window for the current parcel. Labels and acronyms as in Figure 1B. **D)** The cortical areas in which SL was stronger for Hits than Misses displayed in inflated cortical surface. Color indicates the average PLF values in the selected time-window for the current parcel. Acronyms for the brain areas: prCN = precuneus, subPS = subparietal sulcus. Borders and rest of the acronyms as in Figure 1B.

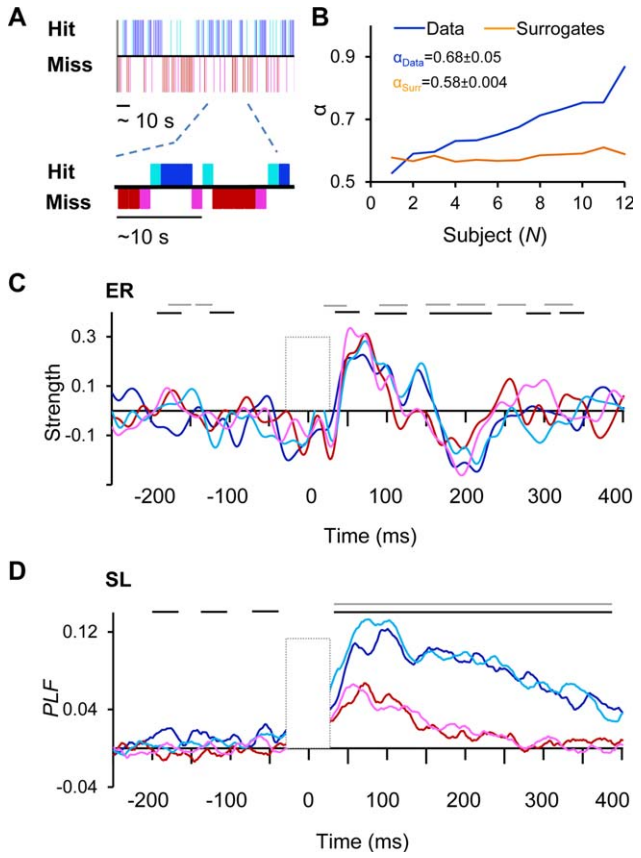

Figure 3.

The strength of ER and SL are not dependent on the position in the Hit-Miss behavioral series. **A)** Behavioral data of 2.5 min from a representative subject showing that behavioral performance is temporally clustered into sequences of Hits (blue) and Misses (red). Different Colors indicate stimulus positions in the behavioral sequence. The last Miss before Hit is indicated with magenta and the first Hit after Miss with cyan. The rest of the Hits are indicated with blue and rest of the Misses with red. **B)** Temporal autocorrelations in the behavioral series as estimated with DFA exponent α displayed separately for each subject as well as exponents for the surrogate data. **C)** The relative strength of ER in the contralateral SI for Hits and Misses separately for stimuli in the different positions in the behavioral sequence. Colors as in A. Black lines indicate statistically significant difference between Hits and Misses in the middle of the sequence and grey lines between the first Hits and last Misses ($P < 0.05$, Wilcoxon signed rank test, FDR corrected). **D)** The relative strengths of SL for Hits and Misses in different positions in the behavioral series as displayed in C.

had a greatest extent in the low-alpha (low-α, 8 − 10 Hz) band. SL for the Misses was centered in the theta- (θ, 4 − 8 Hz) to low-α bands as well as to both low- (10 − 20 Hz) and high β band. The strongest difference in the SL between Hits and Misses were hence observed in the delta and low-alpha bands, but observed also in the beta-band. Interestingly, in the low-α band, SL was sustained until the behavioral response.

During the early time-window of 100 and 300 ms from stimulus onset, SL was stronger for Hits compared with Misses in θ to low-α band in wide-spread cortical areas including SM, dlPFC, vlPFC, and parietal cortices of FP and DAN, but also in aCi and mCi of DMN and VAN. During the later time-window of 300 to 500 ms stimulus onset, sustained low-α band SL was stronger for Hits than for Misses in the same areas although not as extensively as during the early time-window (Fig. 5B). In the high-β band, SL was stronger for the Hits than Misses in the SI, SII, SMA, as well as in mFG of FP and in sFG of DMN. Importantly, unlike ERs, SL extended to most anterior parts of the frontal cortex both in low-α and β bands.

We then characterized oscillation amplitude modulations induced by consciously perceived and unperceived stimuli in the TF domain. Both Hits and Misses were characterized by δ−θ-band amplitude increase likely reflecting ER and a subsequent wide-band suppression from α (8 − 12 Hz) to mid-gamma (<40 Hz) frequencies (Fig. 6A). These modulations were also larger for the consciously perceived than for unperceived trials. In addition, early increase in β band amplitudes was stronger for the Hits than Misses. Taken that the mean RT was ∼400 ms, the large-scale amplitude suppression likely reflected the motor preparation and action. Stronger δ−θ-band amplitudes for the Hits than Misses were observed throughout SM and FP networks as well as in intPS of DAN, while low-β band amplitudes were stronger for the Hits than Misses in right-hemispheric SMA, iFS, and intPS of the DAN and in distributed visual areas. During the later time-window α−β amplitudes were suppressed throughout SM, FP, DA, and VA networks (Fig. 6B).

DISCUSSION

In this study, we identified cortical areas where evoked responses (ERs), phase-locking to stimulus onset (SL), as well as induced neuronal oscillations predicted the conscious perception of weak somatosensory stimuli. We observed that somatosensory awareness was predicted by robust and wide-spread SL observed at very early latencies and sustained until the behavioral response together with less extensive and slightly later modulations in the strength of ER and induced oscillation amplitudes. Importantly, we observed that the strength of SL and to a lesser extend also that of ER were correlated with conscious somatosensory perception in somatosensory, lateral prefrontal, posterior parietal, and cingulate cortices and thereby in cortical areas belonging functionally to FP, DAN and SM, but as well as to VAN or DMN as defined by functional connectivity in fMRI recordings [Yeo et al., 2011].

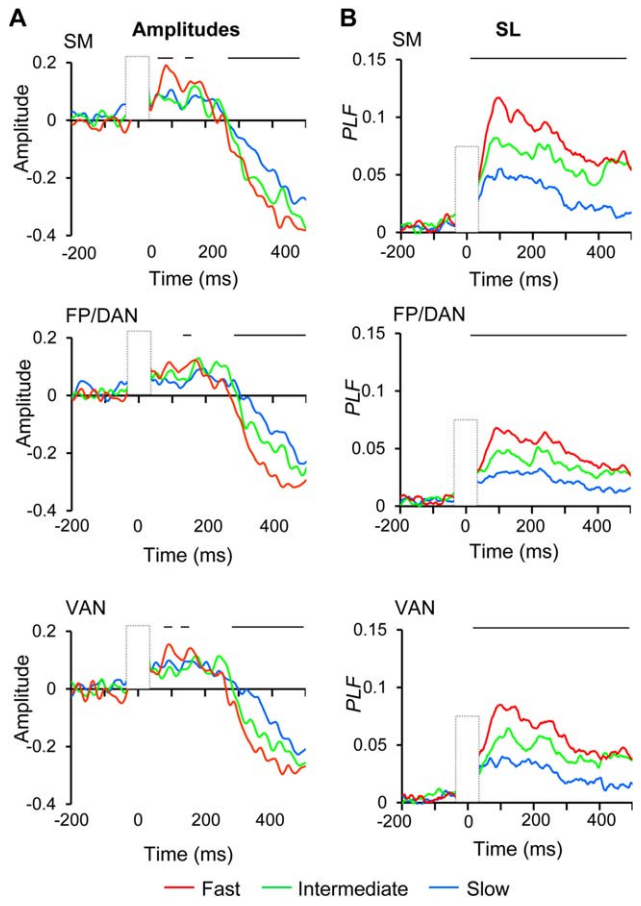

Figure 4.

The strengths of broad-band amplitude and SL are correlated with RTs. **A)** Oscillation amplitudes averaged over SM, FP/DAN, and VAN separately for trials with fast, intermediate, and slow RTs. Lines above indicate significant difference between fast and slow RT trials (Wilcoxon signed ranked test, $P < 0.05$, corrected) **B)** SL as in A.

The Strength of Stimulus Processing in Sensory and FP Areas is Predictive of Conscious Perception

We observed that the strength of ER, as well as broad-band SL and -amplitude were predictive of subsequent somatosensory awareness in the somatosensory areas including both primary (SI) and secondary (SII) somatosensory cortices, and in the lateral PFC including both mFG and sFG of dlPFC and iFG of the vlPFC and hence cortical areas that belong functionally to FP (mFG, iFG) and DMN (sFG). These data corroborate the observations of fMRI studies in which larger activation for consciously perceived than unperceived stimuli is observed in both sensory cortical areas [Bar et al., 2001; Grill-Spector et al., 2000; Hesselmann and Malach, 2011; Hesselmann et al., 2011; Kouider et al., 2007; Polonsky et al., 2000; Tong et al., 1998] and in lateral frontal cortical areas including mFG [Haynes et al., 2005b; Marois et al., 2004] as well as iFG [Vuilleumier et al., 2001] and reveal the time-course and spectral properties of the activation of these areas. Further our data confirm and extend prior MEG data, which have shown that ER in somatosensory cortices [Jones et al., 2007] and SL, ER, and oscillation amplitudes in the MEG sensors over the SM and frontal areas [Palva et al., 2005] predict the conscious perception of threshold level somatosensory stimuli. Prior MEG studies using source reconstruction of neuronal activity have also observed activation of inferior frontal cortex for conscious perception of auditory [Brancucci et al., 2011] and superior frontal cortex for conscious perception of visual [Salti et al., 2015] stimuli suggesting together with our results that all superior, medial, and inferior frontal cortical areas alike might contribute to conscious access of sensory stimuli. Thus, whereas the activity in frontoparietal areas is indeed correlated with conscious perception [Dehaene et al., 2006; Dehaene and Changeux, 2011], it is important to note that cortical regions revealed in electrophysiological recordings to be central in conscious perception are not restricted to functional FP network defined by intrinsic BOLD signal connectivity [Power et al., 2011; Yeo et al., 2011].

Our data also extend prior EEG data which have shown that the strength of ERs are correlated with conscious visual perception [Del Cul et al., 2007; Fahrenfort et al., 2007; Koivisto et al., 2008; Pins and Ffytche, 2003] by identifying the cortical areas in which such correlation take place as well as prior data from iEEG, which have revealed correlation of ERs and oscillation amplitudes with conscious sensory perception in sensory areas [Aru et al., 2012; Fisch et al., 2009; Gaillard et al., 2009; Vidal et al., 2014] by demonstrating that oscillation phase and amplitude dynamics are correlated positively with conscious perception also in frontal and cingulate cortices.

Hence, the present data show that the strength of both SL and ER were stronger for the consciously perceived than for unperceived stimuli also in DAN and thus shows that by using source localization of neuronal activity and co-localization of this activity with functional connectivity networks obtained from fMRI, the attentional component of conscious perception can be dissociated from the other factors that might contribute to NCC in threshold detection tasks [Pitts et al., 2014a; Salti et al., 2015]. As DAN has been indicated a role in attentional orienting [Corbetta and Shulman, 2002; Corbetta et al., 2008], and internal attention [Griffin and Nobre, 2003; Nobre et al., 2004], these data support the view of intertwined mechanisms for sensory awareness and attention [Srinivasan, 2008]. In line with these ideas, a recent transcranial magnetic study has shown that stimulation of frontal eyes fields that is central component of DAN, facilitates conscious visual perception which demonstrates that activity in DAN has a functional significance is shaping conscious access [Chanes et al., 2015].

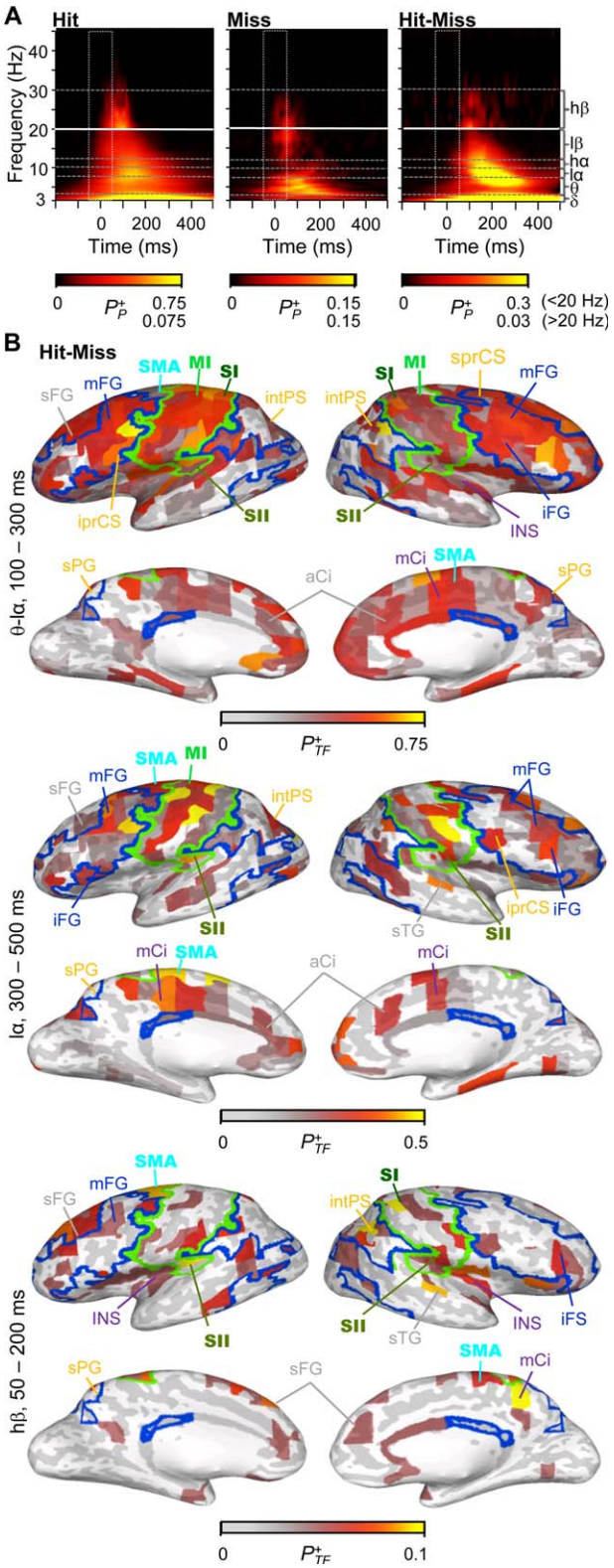

Early NCC for Threshold Level Stimuli

Similarly to prior studies using threshold level sensory stimuli, we observed that the strength of M70 and M130 components of the ER from 70 to 130 ms stimulus onset, respectively, predicted the subsequent conscious perception. However, during M70, differences for the conscious and unconscious stimuli were observed in SII, iFG, an preCS of DAN, while for M130 and M280 ER was stronger for consciously perceived stimuli also in the mFG and sFG of the dlPFC and hence in cortical areas high in neuronal processing hierarchy. These results thus show together with prior studies [Jones et al., 2007; Koivisto et al., 2008; Palva et al., 2005; Pins and Ffytche, 2003] that neuronal activity already at fairly early latencies may facilitate sensory awareness of weak sensory stimuli and differ therefore from those using backward masking to manipulate conscious access and which have observed that the strength of P3 component at 300ms to be correlated with conscious perception [Del Cul et al., 2007; Fahrenfort et al., 2007; Melloni et al., 2011; Sergent et al., 2005]. Such inconsistency in latencies may be explained by experimental differences. Studies using weak sensory stimuli at the threshold of detection reveal the whole cascade of neuronal amplification to those stimuli that are consciously perceived, including the early feed-forward sweep of neuronal activation which by itself cannot be the substrate of sensory awareness [Lamme, 2006; Lamme and Roelfsema, 2000; van Gaal and Lamme, 2012], and which is not observed in backward masking studies revealing later neuronal processing hierarchies [Breitmeyer, 2015].

Although the early feed-forward cascade of neuronal activity is not sufficient for conscious perception to emerge [Lamme, 2006; Lamme and Roelfsema, 2000; van Gaal and Lamme, 2012], our data show that neuronal processing at this early processing stage may differ to consciously perceived and unperceived stimuli and be one of the constituents of the subsequent somatosensory awareness. The early onset latencies of NCC in our study are in line with observations showing that in addition to poststimulus neuronal correlates of awareness, also prestimulus patterns of oscillation amplitudes observed in MEG or EEG recordings in the visual [Wyart and Tallon-Baudry, 2009],

Figure 5.
Spectral characteristics of SL. **A)** Time-frequency representation (TFR) of narrow-band SL. The color scale shows the fraction of brain parcels that were positively (P^+_P) modulated (Wilcoxon signed rank test, $P < 0.01$, FDR corrected) as the function of time and frequency for Hits (left), Misses (middle) and for their difference (right). **B)** The cortical regions in which SL was significantly stronger for Hits than for Misses in the selected TF-ROI. The color indicates the positive fraction (P^+_{TF}) of time-frequency elements in which modulation was observed in the selected ROI (Wilcoxon signed rank test, $P < 0.01$, FDR corrected). For labels, borders, and acronyms see Figure 1B.

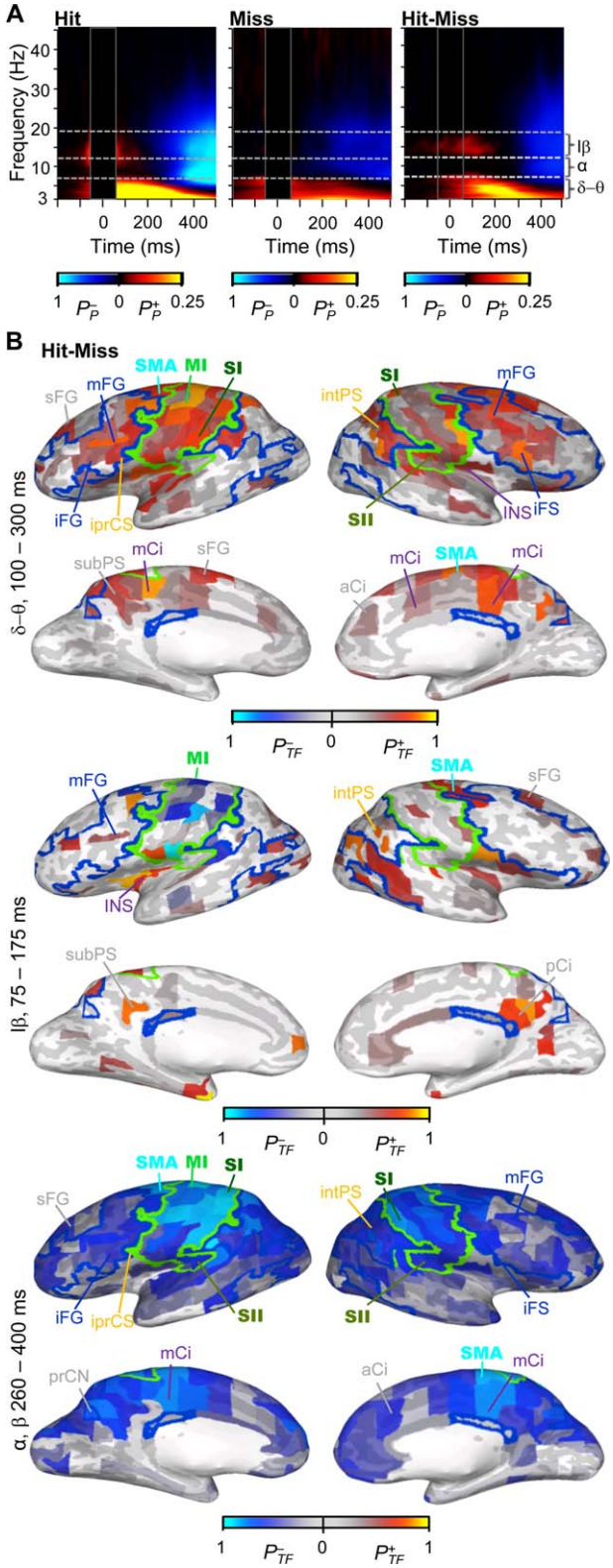

auditory [Sadaghiani et al., 2009], and somatosensory [Jones et al., 2010; Linkenkaer-Hansen et al., 2004; Monto et al., 2008a; Palva et al., 2005; Weisz et al., 2014] modalities are predictive of stimulus subsequent access to awareness. Similar pattern of brain-state dependence has also been observed in invasive recordings from monkey visual cortices in which prestimulus brain-state predict the subsequent conscious perception of visual stimuli [Super et al., 2003].

Neuronal Amplification is not Dependent on the Position in the Behavioral Series

During sustained performance tasks, behavioral performance is clustered into sequences of similar behaviors [Gilden and Wilson, 1995; Monto et al., 2008b; Palva et al., 2013; Verplanck et al., 1952], which often show long-range temporal auto-correlations typical for critical systems [Gilden, 2001; Kello et al., 2010; Monto et al., 2008a; Palva et al., 2013; Thornton and Gilden, 2005; Torre et al., 2011]. Such clustering of the behavioral Hit-Miss series as well long-range auto-correlations in this time-series in the range of critical dynamics were also observed in the present study showing that behavior in the present task operates at the critical state.

In addition, our prior results have shown that detection of these stimuli is also correlated with the phase of infra-slow fluctuations (IFS) (<0.01 Hz) which also modulate the amplitude of fast oscillations and which may reflect fluctuations among task-positive and task-negative networks [Monto et al., 2008a]. As the phase of infra-slow fluctuations could predict gradual increase in the strength of ER and SL as a function of ISF cycle position, we thus asked whether the strength of ER and SL was correlated with the stimulus position in the Hit-Miss cluster. We did not, however, observe any signs of a gradual increase in the strength of these measures as a function of the behavioral Hit-Miss sequence, which is in agreement with prior data in which conscious perception is evidenced by sharp sigmoidal shape of the psychometric functions [Del Cul et al., 2007; Sergent and Dehaene, 2004a] and highly nonlinear responses in fMRI BOLD signal in primary sensory areas [Haynes et al., 2005a; Polonsky et al., 2000], ER signal in EEG sensor level analyses [Del Cul et al., 2007;

Figure 6.
Spectral characteristics of induced amplitude modulations. **A)** TFR of the oscillation amplitude modulations for Hits, Misses and for their difference. The color scale shows the fraction of brain areas in which amplitudes were positively (P^+_P) or negatively (P^-_P) modulated (Wilcoxon signed rank test, $P < 0.05$, corrected). **B)** The cortical areas in which oscillation amplitudes were stronger for Hits than for Misses. Color indicates positive (P^+_{TF}) or negative (P^-_{TF}) fraction of time-frequency elements in which modulation was observed in the selected TF-ROI (Wilcoxon signed rank test, $P < 0.05$, FDR corrected). For labels, borders, and acronyms see Figure 1B.

Sergent and Dehaene, 2004b], and gamma power in iEEG recordings [Fisch et al., 2009]. These data together provides evidence for that the emergence of conscious perception is an all-or-none neuronal phenomenon in wide-spread brain areas and in several temporal scales [Baars, 1988; Dehaene et al., 2006; Tononi and Edelman, 1998]. Thereby, our results indicate that although infra-slow fluctuations are predictive of stimulus subsequent access to consciousness [Monto et al., 2008a], the slow time-scale of these ISF is not reflected in the strength of poststimulus processing. Infra-slow fluctuations together with other prestimulus patterns of neuronal activity may, however, help to exceed a threshold for amplification of neuronal processing and thereby facilitate the subsequent conscious sensory perception.

Robust SL is the Most Prominent Correlate of Conscious Somatosensory Perception

Intriguingly, while we observed broad-band SL to be correlated with conscious perception in wide-spread cortical areas, ER and broad-band amplitude were correlated with conscious perception in more distributed brain areas in these same functional systems. Furthermore, SL was observed in both dlPFC and vlPFC to extend to the most anterior frontal regions which are at the highest level of frontal processing hierarchy [Fuster, 2000; Koechlin et al., 2003], while ER was correlated with conscious perception only in dorsal portion of the dlPFC including parcels of both FP and DAN. These data suggest that specifically the phase-dynamics are crucial in the shaping the emergence of conscious sensory perception perhaps by regulating the information flow across brain areas or by stabilizing neuronal activity as suggested recently for consciously perceived threshold level stimuli [Schurger et al., 2015]. We also observed that the strength of SL in the frontal cortical areas was correlated with conscious perception earlier than that of the amplitude or ER in which the correlates of conscious perception were observed at later latencies from 130 to 140 ms from stimulus onset, suggesting that reorganizing of the phase-dynamics might precede subsequent modulations in the strength of ERs and induced amplitudes. In addition to these effects and in contrast to induced broad-band amplitude, the strength of SL was also robustly and positive correlated with RTs and was stronger for trials with fast compared with slow RTs. These data further demonstrates that SL is behaviorally significant phenomenon and that strong SL speeds up conscious stimulus processing.

Sustained Delta and Theta/Alpha-Band SL in Wide-Spread Cortical Areas is Correlated with Conscious Perception

The analyses of spectral characteristics of SL and oscillation amplitudes revealed that delta/theta- and transient beta-band amplitude increase together with delta, theta-alpha, and transient beta band SL were correlated with sensory awareness. The wide-band components in both amplitudes and SL likely reflected the same phenomena to that of ERs. Intriguingly, both delta as well as low-alpha band SL was sustained until the behavioral response and were not observed for the unperceived trials. Therefore, delta and low-alpha band phase dynamics may be essential components for the subsequent conscious perception of weak threshold level stimuli. Importantly, phase dynamics in both delta [Besle et al., 2011; Schroeder and Lakatos, 2009] as well as in alpha [Drewes and Vanrullen, 2011; Dugue et al., 2011] bands have been shown to regulate neuronal excitability fluctuations and thereby to support sensory perception of attended information. Alpha- and beta-band synchronization between SI and iFG has also been shown to suppress processing of non-attended somatosensory stimuli [Sacchet et al., 2015]. Hence, in our task delta- and alpha band phase-dynamics might regulate information flow across cortical areas and thereby support the emergence of conscious awareness.

Importantly, both delta- and theta/alpha bands SL was observed in wide-spread cortical regions, in particular in SM, cingulate cortex, as well as in FP and DAN extending to the most anterior portions of the frontal cortex and which belong to DMN [Power et al., 2011; Yeo et al., 2011]. Anterior frontal areas are thought to underlie the most complex human behaviors [Fuster, 2008] and have been associated with conscious sensory perception also in prior studies [Boly et al., 2007; Sadaghiani et al., 2009; Turatto et al., 2004]. The strong SL in frontal cortex suggests that phase reorganization of neuronal activity in this area is a crucial constituent for the rise of conscious sensory perception.

In contrast to SL, in our data, oscillation amplitudes were not as strongly correlated with conscious perception. Delta as well as transient beta band increase was strongest in SII and observed only in few dorsal parcels of the dlPFC. The lack of strong oscillation amplitude modulations specific to consciously perceived stimuli other than in delta band might be caused by the very simple and weak sensory stimuli used in the study and of which processing might not involve gamma-band activity often observed to be correlated with conscious sensory perception [Aru et al., 2012; Fisch et al., 2009; Gaillard et al., 2009; Schurger et al., 2006; Vidal et al., 2014; Wyart and Tallon-Baudry, 2008]. Thereby these results support the view in which contents of conscious sensory perception are distinct from awareness itself [Aru et al., 2012; Pitts et al., 2014b; Vidal et al., 2015].

The Role of Default Mode and Salience Network in Conscious Perception

In addition to sensory systems, FP, and DAN, we observed early broad-band and sustained theta–alpha-band SL as well as strengthened amplitudes also in the

insular and mid-cingulate structures that belong to VAN or salience networks as well as in the anterior and posterior cingulate and sFG which belong to DMN [Dosenbach et al., 2008; Power et al., 2011; Yeo et al., 2011]. Importantly, prior fMRI studies have observed that the BOLD signal in posterior cingulate is positively correlated with conscious detection of auditory stimuli [Sadaghiani et al., 2009], while the BOLD signal in anterior cingulate is positively correlated with conscious visual perception [Dehaene et al., 2003; Marois et al., 2004]. Intriguingly, a recent study observed that neuronal oscillations in a cingulate cortex were locked to heart beats and that this correlation was predictive of conscious sensory perception [Park et al., 2014]. Further, the activity in these areas has been associated with egocentric bodily sensations [Nagels et al., 2015], processing of emotions [Paulus et al., 2015] as well as monitoring of cognitive goals and expectations [Michelet et al., 2015; Sheth et al., 2012]. Thereby, modulations of neuronal activity in cingulate cortices might be a crucial constituent in the subjective experience of conscious sensory perception.

ACKNOWLEDGMENT

The authors thank Drs. Simo Monto and J. Matias Palva for comments on an earlier version of the manuscript.

REFERENCES

Aru J, Axmacher N, Do Lam AT, Fell J, Elger CE, Singer W, Melloni L (2012): Local category-specific gamma band responses in the visual cortex do not reflect conscious perception. J Neurosci 32:14909–14914.

Auksztulewicz R, Blankenburg F (2013): Subjective rating of weak tactile stimuli is parametrically encoded in event-related potentials. J Neurosci 33:11878–11887.

Baars BJ (1988): A Cognitive Theory of Consciousness. Cambridge: Cambridge University Press. pp 448.

Bar M, Tootell RB, Schacter DL, Greve DN, Fischl B, Mendola JD, Rosen BR, Dale AM (2001): Cortical mechanisms specific to explicit visual object recognition. Neuron 29:529–535.

Bell AJ, Sejnowski TJ (1995): An information-maximization approach to blind separation and blind deconvolution. Neural Comput 7:1129–1159.

Besle J, Schevon CA, Mehta AD, Lakatos P, Goodman RR, McKhann GM, Emerson RG, Schroeder CE (2011): Tuning of the human neocortex to the temporal dynamics of attended events. J Neurosci 31:3176–3185.

Boly M, Balteau E, Schnakers C, Degueldre C, Moonen G, Luxen A, Phillips C, Peigneux P, Maquet P, Laureys S (2007): Baseline brain activity fluctuations predict somatosensory perception in humans. Proc Natl Acad Sci USA 104:12187–12192.

Boly M, Garrido MI, Gosseries O, Bruno MA, Boveroux P, Schnakers C, Massimini M, Litvak V, Laureys S, Friston K (2011): Preserved feedforward but impaired top-down processes in the vegetative state. Science 332:858–862.

Brancucci A, Franciotti R, D'Anselmo A, Della Penna S, Tommasi L (2011): The sound of consciousness: Neural underpinnings of auditory perception. J Neurosci 31:16611–16618.

Breitmeyer BG (2015): Psychophysical "blinding" methods reveal a functional hierarchy of unconscious visual processing. Conscious Cogn 35:234–250.

Cardin JA, Carlen M, Meletis K, Knoblich U, Zhang F, Deisseroth K, Tsai LH, Moore CI (2009): Driving fast-spiking cells induces gamma rhythm and controls sensory responses. Nature 459: 663–667.

Chanes L, Quentin R, Vernet M, Valero-Cabre A (2015): Arrhythmic activity in the left frontal eye field facilitates conscious visual perception in humans. Cortex 71:240–247.

Corbetta M, Patel G, Shulman GL (2008): The reorienting system of the human brain: From environment to theory of mind. Neuron 58:306–324.

Corbetta M, Shulman GL (2002): Control of goal-directed and stimulus-driven attention in the brain. Nat Rev Neurosci 3: 201–215.

Dale AM, Fischl B, Sereno MI (1999): Cortical surface-based analysis. I. Segmentation and surface reconstruction. Neuroimage 9: 179–194.

Dale AM, Liu AK, Fischl BR, Buckner RL, Belliveau JW, Lewine JD, Halgren E (2000): Dynamic statistical parametric mapping: Combining fMRI and MEG for high-resolution imaging of cortical activity. Neuron 26:55–67.

Dehaene S, Artiges E, Naccache L, Martelli C, Viard A, Schurhoff F, Recasens C, Martinot ML, Leboyer M, Martinot JL (2003): Conscious and subliminal conflicts in normal subjects and patients with schizophrenia: The role of the anterior cingulate. Proc Natl Acad Sci USA 100:13722–13727.

Dehaene S, Changeux JP (2011): Experimental and theoretical approaches to conscious processing. Neuron 70:200–227.

Dehaene S, Changeux JP, Naccache L, Sackur J, Sergent C (2006): Conscious, preconscious, and subliminal processing: A testable taxonomy. Trends Cogn Sci 10:204–211.

Del Cul A, Baillet S, Dehaene S (2007): Brain dynamics underlying the nonlinear threshold for access to consciousness. PLoS Biol 5:e260.

Del Cul A, Dehaene S, Reyes P, Bravo E, Slachevsky A (2009): Causal role of prefrontal cortex in the threshold for access to consciousness. Brain 132:2531–2540.

Destrieux C, Fischl B, Dale A, Halgren E (2010): Automatic parcellation of human cortical gyri and sulci using standard anatomical nomenclature. Neuroimage 53:1–15.

Dosenbach NU, Fair DA, Cohen AL, Schlaggar BL, Petersen SE (2008): A dual-networks architecture of top-down control. Trends Cogn Sci 12:99–105.

Drewes J, Vanrullen R (2011): This is the rhythm of your eyes: The phase of ongoing electroencephalogram oscillations modulates saccadic reaction time. J Neurosci 31:4698–4708.

Dugue L, Marque P, VanRullen R (2011): The phase of ongoing oscillations mediates the causal relation between brain excitation and visual perception. J Neurosci 31:11889–11893.

Fahrenfort JJ, Scholte HS, Lamme VA (2007): Masking disrupts reentrant processing in human visual cortex. J Cogn Neurosci 19:1488–1497.

Fisch L, Privman E, Ramot M, Harel M, Nir Y, Kipervasser S, Andelman F, Neufeld MY, Kramer U, Fried I, Malach R (2009): Neural "ignition": Enhanced activation linked to perceptual awareness in human ventral stream visual cortex. Neuron 64: 562–574.

Fischl B, Salat DH, Busa E, Albert M, Dieterich M, Haselgrove C, van der Kouwe A, Killiany R, Kennedy D, Klaveness S, Montillo A, Makris N, Rosen B, Dale AM (2002): Whole brain

segmentation: Automated labeling of neuroanatomical structures in the human brain. Neuron 33:341–355.
Fuster JM (2008): The Prefrontal Cortex. London, UK: Academic Press. Elsevier Ltd.
Fuster JM (2000): Executive frontal functions. Exp Brain Res 133: 66–70.
Gaillard R, Dehaene S, Adam C, Clemenceau S, Hasboun D, Baulac M, Cohen L, Naccache L (2009): Converging intracranial markers of conscious access. PLoS Biol 7:e61.
Gilden DL (2001): Cognitive emissions of 1/f noise. Psychol Rev 108:33–56.
Gilden DL, Wilson SG (1995): On the nature of streaks in signal detection. Cognit Psychol 28:17–64.
Griffin IC, Nobre AC (2003): Orienting attention to locations in internal representations. J Cogn Neurosci 15:1176–1194.
Grill-Spector K, Kushnir T, Hendler T, Malach R (2000): The dynamics of object-selective activation correlate with recognition performance in humans. Nat Neurosci 3:837–843.
Hämäläinen MS, Ilmoniemi RJ (1994): Interpreting magnetic fields of the brain: Minimum norm estimates. Med Biol Eng Comput 32:35–42.
Hämäläinen MS, Sarvas J (1989): Realistic conductivity geometry model of the human head for interpretation of neuromagnetic data. IEEE Trans Biomed Eng 36:165–171.
Haynes JD, Deichmann R, Rees G (2005a): Eye-specific effects of binocular rivalry in the human lateral geniculate nucleus. Nature 438:496–499.
Haynes JD, Driver J, Rees G (2005b): Visibility reflects dynamic changes of effective connectivity between V1 and fusiform cortex. Neuron 46:811–821.
Hesselmann G, Hebart M, Malach R (2011): Differential BOLD activity associated with subjective and objective reports during "blindsight" in normal observers. J Neurosci 31:12936–12944.
Hesselmann G, Malach R (2011): The link between fMRI-BOLD activation and perceptual awareness is "stream-invariant" in the human visual system. Cereb Cortex 21:2829–2837.
Honkanen R, Rouhinen S, Wang SH, Palva JM, Palva S (2014): Gamma oscillations underlie the maintenance of feature-specific information and the contents of visual working memory. Cereb Cortex 25:3788–3801.
Jones SR, Kerr CE, Wan Q, Pritchett DL, Hamalainen M, Moore CI (2010): Cued spatial attention drives functionally relevant modulation of the mu rhythm in primary somatosensory cortex. J Neurosci 30:13760–13765.
Jones SR, Pritchett DL, Stufflebeam SM, Hamalainen M, Moore CI (2007): Neural correlates of tactile detection: A combined magnetoencephalography and biophysically based computational modeling study. J Neurosci 27:10751–10764.
Kello CT, Brown GD, Ferrer-I-Cancho R, Holden JG, Linkenkaer-Hansen K, Rhodes T, Van Orden GC (2010): Scaling laws in cognitive sciences. Trends Cogn Sci 14:223–232.
Koechlin E, Ody C, Kouneiher F (2003): The architecture of cognitive control in the human prefrontal cortex. Science 302:1181–1185.
Koivisto M, Lahteenmaki M, Sorensen TA, Vangkilde S, Overgaard M, Revonsuo A (2008): The earliest electrophysiological correlate of visual awareness? Brain Cogn 66:91–103.
Korhonen O, Palva S, Palva JM (2014): Sparse weightings for collapsing inverse solutions to cortical parcellations optimize M/EEG source reconstruction accuracy. J Neurosci Methods 226:147–160.
Kouider S, Dehaene S, Jobert A, Le Bihan D (2007): Cerebral bases of subliminal and supraliminal priming during reading. Cereb Cortex 17:2019–2029.
Lamme VA (2006): Towards a true neural stance on consciousness. Trends Cogn Sci 10:494–501.
Lamme VA, Roelfsema PR (2000): The distinct modes of vision offered by feedforward and recurrent processing. Trends Neurosci 23:571–579.
Linkenkaer-Hansen K, Nikulin VV, Palva S, Ilmoniemi RJ, Palva JM (2004): Prestimulus oscillations enhance psychophysical performance in humans. J Neurosci 24:10186–10190.
Marois R, Yi DJ, Chun MM (2004): The neural fate of consciously perceived and missed events in the attentional blink. Neuron 41:465–472.
Melloni L, Schwiedrzik CM, Muller N, Rodriguez E, Singer W (2011): Expectations change the signatures and timing of electrophysiological correlates of perceptual awareness. J Neurosci 31:1386–1396.
Michelet T, Bioulac B, Langbour N, Goillandeau M, Guehl D, Burbaud P (2015): Electrophysiological correlates of a versatile executive control system in the monkey anterior cingulate cortex. Cereb Cortex. Epub ahead of print. doi:10.1093/cercor/bhv004
Monto S, Palva S, Voipio J, Palva JM (2008): Very slow EEG fluctuations predict the dynamics of stimulus detection and oscillation amplitudes in humans. J Neurosci 28:8268–8272.
Nagels A, Kircher T, Steines M, Straube B (2015): Feeling addressed! The role of body orientation and co-speech gesture in social communication. Hum Brain Mapp 36:1925–1936.
Nobre AC, Coull JT, Maquet P, Frith CD, Vandenberghe R, Mesulam MM (2004): Orienting attention to locations in perceptual versus mental representations. J Cogn Neurosci 16: 363–373.
Palva JM, Monto S, Kulashekhar S, Palva S (2010): Neuronal synchrony reveals working memory networks and predicts individual memory capacity. Proc Natl Acad Sci USA 107:7580–7585.
Palva JM, Palva S (2011): Roles of multiscale brain activity fluctuations in shaping the variability and dynamics of psychophysical performance. Prog Brain Res 193:335–350.
Palva JM, Palva S (2012): Infra-slow fluctuations in electrophysiological recordings, blood-oxygenation-level-dependent signals, and psychophysical time series. Neuroimage 62:2201–2211.
Palva JM, Zhigalov A, Hirvonen J, Korhonen O, Linkenkaer-Hansen K, Palva S (2013): Neuronal long-range temporal correlations and avalanche dynamics are correlated with behavioral scaling laws. Proc Natl Acad Sci USA 110:3585–3590.
Palva S, Kulashekhar S, Hamalainen M, Palva JM (2011): Localization of cortical phase and amplitude dynamics during visual working memory encoding and retention. J Neurosci 31:5013–5025.
Palva S, Linkenkaer-Hansen K, Naatanen R, Palva JM (2005): Early neural correlates of conscious somatosensory perception. J Neurosci 25:5248–5258.
Park HD, Correia S, Ducorps A, Tallon-Baudry C (2014): Spontaneous fluctuations in neural responses to heartbeats predict visual detection. Nat Neurosci 17:612–618.
Paulus FM, Krach S, Blanke M, Roth C, Belke M, Sommer J, Muller-Pinzler L, Menzler K, Jansen A, Rosenow F, Bremmer F, Einhauser W, Knake S (2015): Fronto-insula network activity explains emotional dysfunctions in juvenile myoclonic epilepsy: Combined evidence from pupillometry and fMRI. Cortex 65:219–231.
Pins D, Ffytche D (2003): The neural correlates of conscious vision. Cereb Cortex 13:461–474.

Pitts MA, Padwal J, Fennelly D, Martinez A, Hillyard SA (2014): Gamma band activity and the P3 reflect post-perceptual processes, not visual awareness. Neuroimage 101:337–350.

Polonsky A, Blake R, Braun J, Heeger DJ (2000): Neuronal activity in human primary visual cortex correlates with perception during binocular rivalry. Nat Neurosci 3:1153–1159.

Power JD, Cohen AL, Nelson SM, Wig GS, Barnes KA, Church JA, Vogel AC, Laumann TO, Miezin FM, Schlaggar BL, Petersen SE (2011): Functional network organization of the human brain. Neuron 72:665–678.

Sacchet MD, LaPlante RA, Wan Q, Pritchett DL, Lee AKC, Hämäläinen M, Moore CI, Kerr CE, Jones SR (2015): Attention drives synchronization of alpha and beta rhythms between right inferior frontal and primary sensory neocortex. J Neurosci 35:2074–2082.

Sadaghiani S, Hesselmann G, Kleinschmidt A (2009): Distributed and antagonistic contributions of ongoing activity fluctuations to auditory stimulus detection. J Neurosci 29:13410–13417.

Sadaghiani S, Poline JB, Kleinschmidt A, D'Esposito M (2015): Ongoing dynamics in large-scale functional connectivity predict perception. Proc Natl Acad Sci USA 112:8463–8468.

Salti M, Monto S, Charles L, King JR, Parkkonen L, Dehaene S (2015): Distinct cortical codes and temporal dynamics for conscious and unconscious percepts. Elife 4:10–7554. /eLife.05652.

Schroeder CE, Lakatos P (2009): Low-frequency neuronal oscillations as instruments of sensory selection. Trends Neurosci 32: 9–18.

Schurger A, Cowey A, Tallon-Baudry C (2006): Induced gamma-band oscillations correlate with awareness in hemianopic patient GY. Neuropsychologia 44:1796–1803.

Schurger A, Sarigiannidis I, Naccache L, Sitt JD, Dehaene S (2015): Cortical activity is more stable when sensory stimuli are consciously perceived. Proc Natl Acad Sci USA 112:E2083–E2092.

Sergent C, Baillet S, Dehaene S (2005): Timing of the brain events underlying access to consciousness during the attentional blink. Nat Neurosci 8:1391–1400.

Sergent C, Dehaene S (2004a): Is consciousness a gradual phenomenon? Evidence for an all-or-none bifurcation during the attentional blink. Psychol Sci 15:720–728.

Sergent C, Dehaene S (2004b): Neural processes underlying conscious perception: experimental findings and a global neuronal workspace framework. J Physiol Paris 98:374–384.

Sheth SA, Mian MK, Patel SR, Asaad WF, Williams ZM, Dougherty DD, Bush G, Eskandar EN (2012): Human dorsal anterior cingulate cortex neurons mediate ongoing behavioral adaptation. Nature 488:218–221.

Singer W (1999): Neuronal synchrony: A versatile code for the definition of relations? Neuron 24: 49–65, 111-125.

Sinkkonen J, Tiitinen H, Naatanen R (1995): Gabor filters: An informative way for analysing event-related brain activity. J Neurosci Methods 56:99–104.

Srinivasan N (2008): Interdependence of attention and consciousness. Prog Brain Res 168:65–75.

Super H, van der Togt C, Spekreijse H, Lamme VA (2003): Internal state of monkey primary visual cortex (V1) predicts figure-ground perception. J Neurosci 23:3407–3414.

Tallon-Baudry C, Bertrand O, Delpuech C, Pernier J (1996): Stimulus specificity of phase-locked and non-phase-locked 40 Hz visual responses in human. J Neurosci 16:4240–4249.

Taulu S, Simola J, Kajola M (2005): Applications of the signal space separation method. IEEE Trans Signal Process 53:3359–3313.

Thornton TL, Gilden DL (2005): Provenance of correlations in psychological data. Psychon Bull Rev 12:409–441.

Tong F, Nakayama K, Vaughan JT, Kanwisher N (1998): Binocular rivalry and visual awareness in human extrastriate cortex. Neuron 21:753–759.

Tononi G, Edelman GM (1998): Consciousness and complexity. Science 282:1846–1851.

Torre K, Balasubramaniam R, Rheaume N, Lemoine L, Zelaznik HN (2011): Long-range correlation properties in motor timing are individual and task specific. Psychon Bull Rev 18:339–346.

Turatto MCA, Sandrini M, Miniussi C (2004): The role of the right dorsolateral prefrontal cortex in visual change awareness. Neuroreport 15:2549–2552.

van Gaal S, Lamme VA (2012): Unconscious high-level information processing: Implication for neurobiological theories of consciousness. Neuroscientist 18:287–301.

Verplanck WS, Collier GH, Cotton JW (1952): Nonindependence of successive responses in measurements of the visual threshold. J Exp Psychol 44:273–282.

Vidal JR, Perrone-Bertolotti M, Kahane P, Lachaux JP (2015): Intracranial spectral amplitude dynamics of perceptual suppression in fronto-insular, occipito-temporal, and primary visual cortex. Front Psychol 5:1545.

Vidal JR, Perrone-Bertolotti M, Levy J, De Palma L, Minotti L, Kahane P, Bertrand O, Lutz A, Jerbi K, Lachaux JP (2014): Neural repetition suppression in ventral occipito-temporal cortex occurs during conscious and unconscious processing of frequent stimuli. Neuroimage 95:129–135.

Vuilleumier P, Sagiv N, Hazeltine E, Poldrack RA, Swick D, Rafal RD, Gabrieli JD (2001): Neural fate of seen and unseen faces in visuospatial neglect: A combined event-related functional MRI and event-related potential study. Proc Natl Acad Sci USA 98: 3495–3500.

Weisz N, Wuhle A, Monittola G, Demarchi G, Frey J, Popov T, Braun C (2014): Prestimulus oscillatory power and connectivity patterns predispose conscious somatosensory perception. Proc Natl Acad Sci USA 111:E417–E425.

Womelsdorf T, Fries P (2007): The role of neuronal synchronization in selective attention. Curr Opin Neurobiol 17:154–160.

Wyart V, Tallon-Baudry C (2008): Neural dissociation between visual awareness and spatial attention. J Neurosci 28:2667–2679.

Wyart V, Tallon-Baudry C (2009): How ongoing fluctuations in human visual cortex predict perceptual awareness: baseline shift versus decision bias. J Neurosci 29:8715–8725.

Yeo BT, Krienen FM, Sepulcre J, Sabuncu MR, Lashkari D, Hollinshead M, Roffman JL, Smoller JW, Zollei L, Polimeni JR, Fischl B, Liu H, Buckner RL (2011): The organization of the human cerebral cortex estimated by intrinsic functional connectivity. J Neurophysiol 106:1125–1165.